

Performance analysis and side lobe suppression in radon-Fourier transform based on random pulse repetition interval

Qian Chen^{1, 2*}, Junhao Liu², Chaowei Fu², Haitao Wang²

¹*School of Information and Electronics, Beijing Institute of Technology, Beijing, 100081, China*

²*Shanghai Radio Equipment Research Institute, Shanghai, 200090, China*

Received 1 June 2014, www.cmnt.lv

Abstract

In order to solve the Blind Speed Side Lobe (BSSL) appeared in Radon-Fourier Transform (RFT) method used for dim target detection, a novel method of BSSL suppression is proposed in this paper. It is based on Random Pulse Repetition Interval (RPRI). The process of RPRI-RFT and the BSSL properties are described, the performance of coherent integration and the modulation noise of RFT algorithm based on RPRI are analysed in detail. Both the theoretical analysis and the numerical experimental results show that RPRI-RFT can be used to improve signal-to-noise ratio (SNR) and suppress BSSL effectively, and the influence of modulation noise of RPRI can be suppressed by the long-time integration characteristic, thus significantly improve the ability of low pulse repetition frequency radar to detect and measure long-range weak high-speed multi-targets.

Keywords: Blind Velocity Side Lobe, Radon-Fourier Transform, Random Pulse Repetition Interval

1 Introduction

With the development of radar stealth technology, the radar cross section (RCS) of target decreases sharply, weakening the energy of radar echo and diminishing the range of radar detection. Long-time integration is an effective method to improve the detection performance of dim targets [1-3]. With the increase of integration time, however, the problem of across range unit (ARU) walk will occur inevitably. Performing directly conventional methods of moving target detection (MTD) on high-velocity targets, the energy of targets spread over multiple resolution units [4-6] and cannot be integrated effectively. In this case, the increase of integration time cannot improve the performance of radar detection.

Non-coherent integration and coherent integration are two basic methods for long-time integration. The former mainly accumulates the energy along with the motion trajectory of targets to solve the problem of ARU. As a typical algorithm, the Hough Transform (HT) proposed by Carlson does not need phase compensation, making it easy to implement [7-9]. However, without phase information, the energy of target cannot be accumulated completely and this method cannot work well in extremely low SNR scenario [10]. The latter has drawn extensive attention from academic community and has been deeply investigated in recently years, because of its better integrated gain in the field of dim target detection. Techniques for ARU compensation in the long-time coherent integration can be classified into two types. In the first type, ARU compensation can be implemented by shifting or expanding the envelope after pulse

compression [11]. In order to guarantee the compensation precision, interpolation in range dimension should be adopted, so the memory cost is huge. In the second type, ARU compensation is realized in the transform domain of the range-pulse plane, such as Keystone transformation, achieving ARU compensation of constant-velocity targets [12-14]. This method is free of searching operation, but it cannot eliminate the ARU effect for multiple targets with different ambiguity number simultaneously.

In recent years, based on the coupling relationship between range walk and Doppler frequency, Radon-Fourier Transform (RFT) is proposed to realize the long-time coherent integration [15-17] by mapping the echo pulse to the range-Doppler plane. RFT concentrating the energy to a focused peak, improves the radar detection performance of dim targets. However, because of the discrete pulse sampling, finite range resolution and limited integration time, the BSSL still exists in the case of Low Pulse Repetition Frequency (LPRF). Since the BSSL would increase the ratio of false alarm and deteriorate the detection performance, a symmetrical weighting method has been proposed to suppress the BSSL in RFT integration plane. The locations of BSSLs can be controlled via different weighting functions, and the BSSLs can be eliminated by combing the different weighted RFT results [16]. However, BSSLs still cannot be eliminated completely when the BSSLs appear simultaneously in both RFT outputs. Another method based on the design of pulse repetition interval (PRI) has been proposed in Ref. [18]. By jointly processing the RFT outputs in two adjacent Coherent Processing Intervals (CPIs), minimum criterion is employed between

* *Corresponding author* e-mail 3241126@qq.com

the two different PRI to achieve BSSL suppression. It should be note that the algorithm needs at least two CPIs, so that the integration time is increased twice and the radar efficiency is halved. A BSSL suppression method based on CLEAN algorithm has been proposed in [19]. The peak position of echo envelope is first obtained after RFT operation, and according to the relationship among BSSL, velocity and range, the positions of BSSL are confirmed and removed. And then the RFT peak will be determined. Though the BSSL of one target can be well restrained, the target cannot be detected when its main lobe overlaps the BSSL of another target.

In this paper, a novel RFT algorithm based on Random Pulse Repetition Interval (RPRI) is proposed to suppress BSSL. And the paper is organized as follows: the principle of RFT algorithm is analysed, and the causes of BSSL of discrete RFT are presented in section 2. In section 3, the RFT algorithm based on RPRI is proposed, and the analyses about the modulation noise and BSSL suppression performance of RFT algorithm are presented. In section 4, the simulation results of the proposed method are shown. Finally, the conclusions are given out in section 5.

2 The characteristics of RFT

2.1 SIGNAL MODEL

Suppose a linear frequency modulation (LFM) signal $p(t)$ is used by the radar transmitting, i.e.,

$$p(t) = \text{rect}(t/T_p) \exp(j\pi\gamma t^2), \quad (1)$$

where T_p is the pulse duration, γ is the modulation frequency rate, and $\text{rect}(\bullet)$ is the rectangular function.

For a point target with the RCS of Swerling-0 type, the received echo signal can be written as

$$s_r(\hat{t}, t_m) = A_t p(\hat{t} - 2r(t_m)/c) \exp(-j4\pi f_c r(t_m)/c), \quad (2)$$

where \hat{t} and t_m ($t_m = mT_r$, T_r is the PRI) denote the quick-time and slow-time respectively, f_c is the carrier frequency, c represents the light velocity and A_t is the amplitude of target. It is supposed that the radial velocity of the target is uniform. The instantaneous distance between radar and target can be expressed as $r(t_m) = r_0 + v_0 t_m$ where r_0 is the initial distance from radar platform to target, and v_0 is the radial velocity of target.

After range compression, the echo signal can be represented as

$$s_{r,M}(\hat{t}, t_m) = A_0 \text{sinc}\left(B(\hat{t} - 2(r_0 + v_0 t_m)/c)\right) \cdot \exp(-j4\pi f_c r_0/c) \exp(-j4\pi f_c v_0 t_m/c), \quad (3)$$

where A_0 is the amplitude of baseband signal, B is the bandwidth of LFM signal.

For the conventional MTD method, echo envelop is supposed to be in the same range unit, and the coherent integration results can be written as

$$S_p(t, v) = \int_{T_{CPI}} s_{r,M}(\hat{t}, t_m) \exp(j4\pi v t_m/\lambda) dt_m, \quad (4)$$

where λ is the wavelength, $S_p(t, v)$ is the coherent integration result in the range-velocity plane.

In equation (4), the pulse integration time should satisfy

$$T_{CPI} \leq \frac{\rho_r}{v_{\max}}, \quad (5)$$

where ρ_r is the range resolution, and $\rho_r = c/(2B)$.

However, in general cases, the maneuvering targets cannot satisfy (5) during the long integration time, so ARU will appear, thus affecting the coherent integration of energy. RFT algorithm is a solution way to deal with the effect of ARU. For uniform velocity motion, it can be expressed as

$$G(r, v) = \int s_{r,M}\left(\frac{2(r + vt_m)}{c}, t_m\right) \exp\left(j\frac{4\pi vt_m}{\lambda}\right) dt_m, \quad (6)$$

Equation (6) shows that the echo envelope of each slow-time is extracted along with the motion track $r(t_m) = r_0 + v_0 t_m$, and the phase terms are compensated based on the relationship between velocity and Doppler frequency. In contrast, equation (4) shows that the sample points are extracted in the same range cell for different pulse repetition interval. Therefore, RFT can integrate the energy of target completely, while MTD cannot. Since motion track of the target is unknown before detection, two-dimensional joint searching of range and velocity is required in the RFT algorithm.

In practical application, the discrete form of (6) can be rewritten as

$$G_D(r, v) = \sum_{m=0}^{M-1} s_{r,M}\left(\text{round}\left(\frac{r + vmT_r}{\rho_r}\right), m\right) \cdot \exp(j4\pi vmT_r/\lambda) = A_0 \sum_{m=0}^{M-1} \text{sinc}\left(2B((r-r_0)+mT_r(v-v_0))/c\right) \cdot \exp(j4\pi(v-v_0)mT_r/\lambda), \quad (7)$$

where M is the number of integrated pulses. The maximum of integration peak can be found by searching in distance-velocity parameters' plane, and the peak value can be written as

$$G(r_0, v_0) = A_0 M. \quad (8)$$

2.2 RFT BSSL CHARACTERISTICS

For LPRI Pulse Doppler (PD) radar, the accumulating gain of MTD method (shown in (4)) at ambiguous frequency point $f_d + k/T_r$, corresponding to the ambiguous velocity $v(k) = v_0 + kv_b$, where $v_b = \lambda/2T_r$ is the blind velocity, is the same with true Doppler frequency point, the true velocity cannot be ascertained. For RFT method from equation (7), although phase fluctuation of ambiguous velocity $v(k)$ can still be compensated completely, only some sampling units can be accumulated effectively according to the false motion track of ambiguous velocity $v(k)$, if they are in the same range unit with the real motion track $r(t_m) = r_0 + v_0 t_m$. The valid integration number L of accumulated pulses, which satisfies the above condition, can be represented as

$$L = \begin{cases} \text{round}(|\rho_r / (v - v_0) T_r|) & v \neq v_0 \\ M & v = v_0 \end{cases} \quad (9)$$

In this case, RFT results can be rewritten as

$$G(r_0, v(k)) = A_0 L_k = \frac{2A_0 \rho_r}{k \lambda} \quad (10)$$

Thus, for LPRI PD radar, one main accumulating peak and several BSSLs are generated in RFT output, and the Primary Lobe-to-Side Lobe Ratio (PSLR) is

$$I_k = 20 \lg \left(\frac{Mk \lambda}{2 \rho_r} \right) \quad (11)$$

For constant wavelength, BSSL is relevant with the ambiguity number k , the number of accumulated pulse M and the distance resolution ρ_r . RFT processing can suppress the effect of MTD method on velocity ambiguity, and the suppression ratio is I_k . But RFT still cannot resolve the velocity ambiguity completely. In the case of multiple targets, the phenomena of false alarms will still exist when BSSLs exceed the threshold.

3 BSSL Suppression of RFT based on RPRI

3.1 PROCESS OF RPRI-RFT

PD radar with RPRI resolves the problem of velocity ambiguity by adding random jitter to uniform PRI, and it shows good performance in anti-interception and anti-electronic-jamming.

In RPRI case, slow-time t_m is random, and it can be represented as

$$t_m = mT_r + d_m = (m + \delta_m)T_r, \quad (12)$$

where δ_m is a jitter of uniform distribution added to the average repetition interval T_r , which satisfies $-0.5 \leq \delta_m \leq 0.5$. Then the discrete expression of RPRI-RFT can be written as

$$G_D(r, v) = \sum_{m=0}^{M-1} s_{r,M} \left(\text{round}((r + vmT_r + vd_m)/\Delta R), m \right) \exp(j4\pi v(mT_r + d_m)/\lambda) \quad (13)$$

Comparing (13) with (7), there are two differences between RPRI-RFT and RFT. First, the envelope delay of the former increases with the random jitter, which is related to d_m instead of increasing linearly with slow-time t_m . When $vd_m \ll \Delta R$, the envelope delay jitter caused by RPRI is much less than the range resolution, and the RPRI can be considered to have no influence on the sampling of envelope. In fact, the condition usually can be satisfied in reality. Secondly, the phase term of RPRI-RFT is not only related to Doppler modulation, but also including a random term $\exp(j4\pi v_0 d_m/\lambda)$, which introduces random noise component to the processing result of RFT. Therefore, RPRI-RFT is equivalent to Non-Uniform Discrete Fourier Transform (NUDFT) along the track of range migration. The Mean and variance of $G_D(r, v)$ are analysed as follows.

The Mean of RPRI-RFT is expressed as

$$\begin{aligned} E(G_D(r, v)) &= E \left(\sum_{m=0}^{M-1} s_{r,M} \left(\text{round}((r + vmT_r)/\rho_r), m \right) \exp \left(j4\pi \frac{v(mT_r + d_m)}{\lambda} \right) \right) \\ &= A_0 E \left\{ \sum_{m=0}^{M-1} \text{sinc} \left(2B(r - r_0) + (mT_r + d_m)(v - v_0)/c \right) \exp \left(j4\pi (v - v_0)(mT_r + d_m)/\lambda \right) \right\} \approx \quad (14) \\ &= A_0 E \left\{ \left(\sum_{m=0}^{M-1} \text{rect} \left((r - r_0) + (mT_r + d_m)(v - v_0)/\rho_r \right) \exp \left(j4\pi (v - v_0)(mT_r + d_m)/\lambda \right) \right) \right\} \approx \\ &= A_0 E \left\{ \sum_{m=0}^{L-1} \exp \left(j4\pi (v - v_0)(mT_r + d_m)/\lambda \right) \right\} \triangleq A_0 x(r, v) \end{aligned}$$

In (14), the condition supported the final approximate equation is $vd_m \ll \rho_r$, that is, the envelope jitter caused by RPRI is far less than the range resolution. As a result, $x(r, v)$ in equation (14) is written as

$$\begin{aligned}
 x(r, v) = & E \left(\sum_{m=0}^{L-1} \exp(j4\pi(v-v_0)(mT_r + d_m)/\lambda) \right) = \\
 & \sum_{m=0}^{L-1} \exp[j4\pi(v-v_0)mT_r/\lambda] \cdot \\
 E \left\{ \exp[j4\pi(v-v_0)d_m/\lambda] \right\} = & \text{sinc}[4(v_0-v)\alpha T_r/\lambda] \cdot \\
 \sum_{m=0}^{L-1} \exp[j4\pi(v-v_0)mT_r/\lambda] = & \text{sinc}[4(v_0-v)\alpha T_r/\lambda] \cdot \\
 L \text{sinc}[2(v_0-v)LT_r/\lambda] \exp[j2\pi(v_0-v)(L-1)T_r/\lambda] & \\
 \text{sinc}[2(v_0-v)T_r/\lambda] &
 \end{aligned} \quad (15)$$

The variance of RPRI-RFT is expressed as

$$\begin{aligned}
 D(G_D(r, v)) = & D \left\{ \sum_{m=0}^{M-1} s_{r,m} \left(\text{round}((r + vmT_r)/\Delta R), m \right) \cdot \right. \\
 & \left. \exp \left(j \frac{4\pi v (mT_r + d_m)}{\lambda} \right) \right\} \quad (16) \\
 = & LA_0^2 \text{sinc}^2(2B(r-r_0)) \{ 1 - \text{sinc}^2(4(v_0-v)\alpha T_r/\lambda) \}
 \end{aligned}$$

In (16), when $v = v_0$, $D(G_D(r_0, v_0)) = 0$, the main integration peak of RPRI-RFT has no noise component. When $v \neq v_0$, $L = \text{round}(|\rho_r / (v - v_0) T_r|)$, however, $D(G_D(r, v))$ becomes smaller with increasing the deviate degree of v from v_0 according to equation (9). From (15) and (16), it can be seen that both the mean and variance of $G_D(r, v)$ have no relationship with the number of integrated pulses M . Therefore, the advantage of RPRI-RFT is that the amplitude of main peak corresponding to target parameter (r_0, v_0) increases with the same proportion as M , while the variance of modulation noise corresponding to other range-velocity parameter points decreases when v deviates from v_0 . Although noise is introduced by random modulation, it is still restrained after RFT processing so that target can be detected in low SNR when M reaches a certain value.

3.2 BSSL PROPERTIES OF RPRI-RFT

For the case of $v = v_0$, $L = M$, $E(G_D(r_0, v_0)) = A_0 M$ and $D(G_D(r_0, v_0)) = 0$, the random modulation has no influence on the integration amplitude of RFT Primary lobe.

The BSSL of RPRI-RFT output is random, and its mean is written as

$$E(G_D(r_0, v(k))) = \frac{2A_0 \rho_r}{k\lambda} \text{sinc}(2\alpha k) \quad (17)$$

Compared with (10), the improvement factor of BSSL for RPRI-RFT can be written as

$$I_a = \text{sinc}(2\alpha k) \quad (18)$$

It can be seen from Equation (18) that, the improvement of BSSL suppression is related to the jitter α and ambiguity number k . Specifically when $\alpha = 0.5$, the mean of BSSL is 0.

The noise variance introduced after RPRI-RFT is computed to be

$$D(G_D(r_0, v(k))) = \frac{2\rho_r A_0^2 (1 - \text{sinc}^2(2\alpha k))}{k\lambda} \quad (19)$$

In this case, PSLR of RPRI-RFT can be rewritten as

$$\bar{I}_k = 10 \lg \left(\frac{M^2}{\left(\frac{4\rho_r^2}{k^2 \lambda^2} - \frac{2\rho_r}{k\lambda} \right) \text{sinc}^2(2\alpha k) + \frac{2\rho_r}{k\lambda}} \right) \quad (20)$$

Equation (20) shows that, PSLR of RPRI-RFT can increase with the increase of M or the jitter α , so the performance of PSLR can be improved effectively by M and α . Formula (19) also shows that BSSL variance will reduce when ambiguity k increases, and however, BSSL variance cannot be completely zero even if $\alpha = 0.5$. Therefore, in order to eliminate BSSL, parameters α and M should be chosen reasonably.

4 Numerical experiments

Numerical simulations are done to verify the above analysis. The parameters of targets and radar are as follows: the radar carrier frequency is 2.5 GHz; the signal bandwidth is 5MHz; the complex sampling frequency is 10MHz; the pulse duration is 10μs; and average repetition frequency is 1 kHz. Three targets are assumed, and their distance and velocity are $T_1(96 \text{ km}, 680 \text{ m/s})$, $T_2(96 \text{ km}, 620 \text{ m/s})$ and $T_3(94 \text{ km}, 680 \text{ m/s})$ respectively.

4.1 UNIFORM PRI PROCESSING

The range walk does not occur when $M = 32$. For uniform PRI, the result of MTD is shown in Figure 1. Velocity ambiguity has emerged on three targets so that the real velocity cannot be obtained correctly. In addition, MTD processing cannot distinguish T_1 from T_2 in the same distance and Doppler unit in Figure 1.

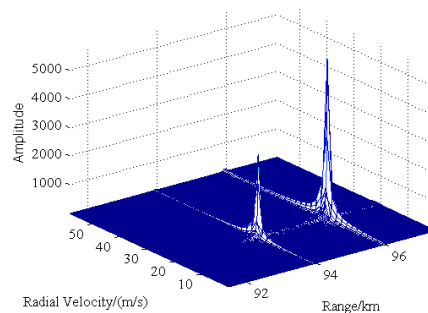


FIGURE 1 MTD results of uniform PRI when M=32

The ARU effect become much more evident when $M = 1024$. The results of MTD and RFT are shown in Figure 2. Figure 2(a) shows that MTD processing cannot distinguish the three targets, because of ARU effect. Figure 2(b) shows that the targets cannot be distinguished because of BSSL, in this case, the PSLR is $I_k = 6.2\text{dB}$.

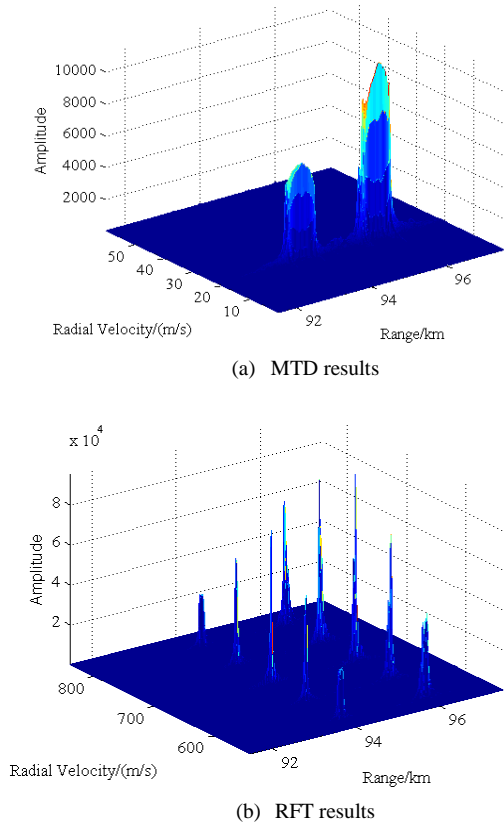
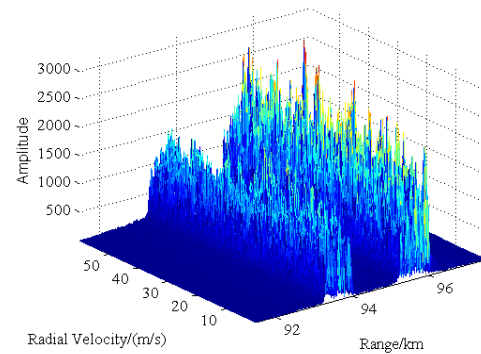


FIGURE 2 Results of uniform PRI when $M = 1024$

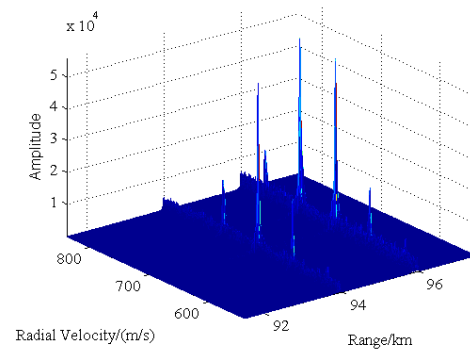
4.2 RESULT OF RPRI-RFT

On the basis of uniform PRI, RPRI status is presented, and the suppression of different jitters on blind side lobe is analysed, which is shown in Figure 3: (1) When $\alpha = 0.3$, MTD shown in Figure 3(a) is directly applied, and the velocity dimension accords with noise distribution; (2) When $\alpha = 0.3$, the RFT processing results are shown in Figure 3(b). The BSSL is further suppressed, and $\bar{I}_1 = 10.9\text{dB}$, which is 4.7dB higher than Figure 2(b); (3) When $\alpha = 0.5$, the RFT processing results are shown in Figure 3(c). The BSSL of RFT is reduced sharply, and the PSLR is $\bar{I}_1 = 27.7\text{dB}$.

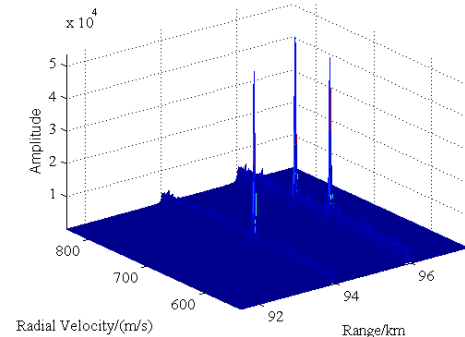
From the above simulation results, it can be observed that the noise does not affect distance resolution along the distance dimension, and the effect of modulation noise is small out of range resolution unit after RPRI-RFT processing; along the velocity dimension, the random modulation noise can be further suppressed, and the influence of modulation noise will be smaller when a certain pulse number M is selected.



(a) MTD results of $\alpha = 0.3$



(b) RPRI-RFT results of $\alpha = 0.3$



(c) RPRI-RFT results of $\alpha = 0.5$

FIGURE 3 Results of RPRI at $M = 1024$

The following Figure 4 shows that PSLR values of different jitter α and the number of accumulated pulse M correspond to the position of the first side lobe.

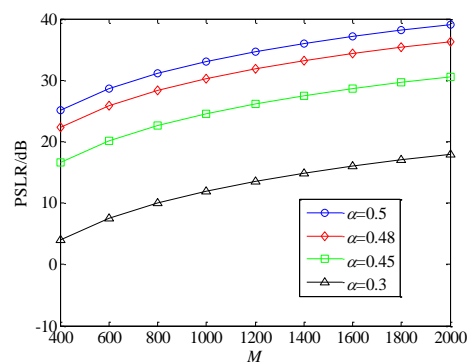
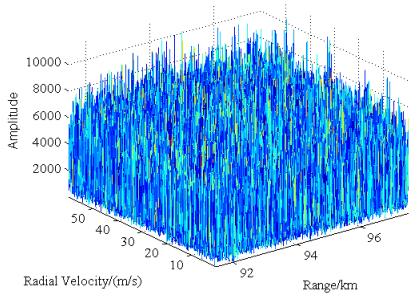


FIGURE 4 PSLR value of different α and M

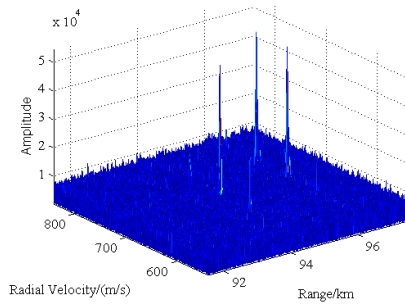
From Figure 4, it shows that the PSLR can be improved to 20 dB when M is more than 600 and $\alpha \geq 0.45$, and the PSLR can be improved to 30 dB when M is more than 1000 and $\alpha \geq 0.48$. These results show different ability to suppress of the BSSL at different parameters.

4.3 PERFORMANCE ANALYSIS OF RPRI-RFT IN LOW SNR

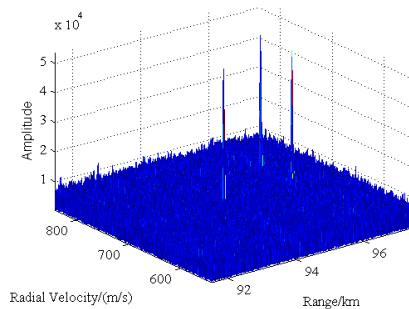
On the basis of section 4.2, Gaussian white noise is introduced, and the input SNR is -20dB. Experimental results are shown in Figure 5. Figure 5(a) shows that targets are submerged in noise after MTD processing. Figure 5(b) shows that signal energy can be integrated so that SNR can be improved substantially after RPRI-RFT processing. Figure 4(c) shows that after the increase of the PRI jitter, BSSL is submerged in noise, and the three pecks of the targets are all much higher than the noise background when the pulse number M is large enough ($M = 1024$), in this case, the output SNR is 20.7dB.



(a) MTD results at $\alpha = 0.3$



(b) RPRI-RFT results at $\alpha = 0.3$



(c) RPRI-RFT results at $\alpha = 0.5$

FIGURE 5 Results of RPRI at M=1024 and SNR=-20dB

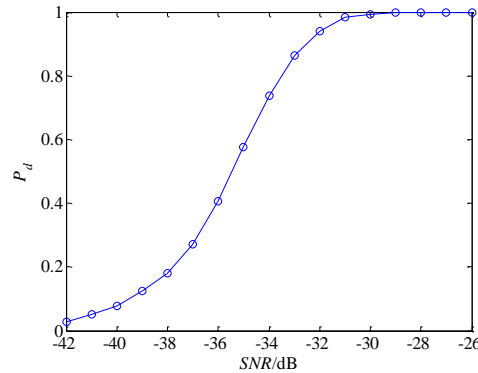


FIGURE 6 Detection performance at different input SNR

In order to analyse the detection performance at low input SNR, the results are given at different input SNR of 1000 Monte-Carlo simulation experiments in Figure 6. With detection probability $P_d = 80\%$ and a given constant false alarm ratio $P_f = 10^{-6}$, Figure 6 shows that the needed input SNR is -34.3dB at RPRI-RFT method.

Simulation results illustrate that RPRI-RFT can be well applied to resolve the problem of dim target detection and anti-velocity ambiguity, thereby achieving accurate velocity and distance of targets.

5 Conclusion

For the detection of the high-velocity dim target, the problem of ARU in long coherent integration time can be solved by RFT algorithm. However, BSSL of RFT algorithm may affect the detection when multiple targets exist in the observed scene. Therefore, a RFT algorithm with RPRI modulation has been proposed to restrain BSSL in this paper. The process of RPRI-RFT has been described and the BSSL properties of RPRI-RFT have been analysed in details. The experimental results have shown that RPRI-RFT can effectively restrain BSSL and the influence of modulation noise of RPRI can be suppressed by the characteristic of long-time integration of RFT. Therefore, the ability to detect long-range and high velocity dim targets has been improved effectively by RPRI-RFT, and proved by the simulation results.

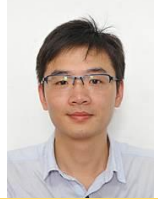
Acknowledgment

This work has been supported in part by Shanghai Aerospace Technology Innovation Fund (Project No. SAST201224).

References

- [1] Skolnik M 2002 Opportunities in radar-2002 *Electronics and Communication Engineering Journal* **14**(6) 263-72
- [2] Cleetus G M 1976 Properties of staggered PRF Radar Spectral Components *IEEE Transaction of Aerospace and Electronic System* **12**(6) 800-3
- [3] Vergara Dominguez L 2004 Analysis of the digital MTI filter with random PRI *IEE Proceedings-F* **140**(2) 129-37
- [4] Barton D K 2004 *Radar System Analysis and Modeling* Beijing: Publishing House of Electronics Industry
- [5] Skolnik M 2002 *Introduction to Radar System* (3rd rd) Columbus, OH: McGraw-Hill
- [6] Yuxi Zhang, Jinping Sun, Bingchen Zhang, Wen Hong 2011 Doppler Ambiguity Resolution Based on Compressive Sensing Theory *Journal of Electronics & Information Technology* **33**(9) 2103-7
- [7] Carlson B D, Evans E D, Wilson S L 1994 Search Radar Detection and Track with the Hough Transform Part I: System Conception *IEEE Transactions on Aerospace and Electronic Systems* **30**(1) 102-8
- [8] Carlson B D, Evans E D, Wilson S L 1994 Search Radar Detection and Track with the Hough Transform Part II: Detection Statistics *IEEE Transactions on Aerospace and Electronic Systems* **30**(1) 109-15
- [9] Carlson B D, Evans E D, Wilson S L 1994 Search Radar Detection and Track with the Hough Transform Part III: Detection Performance with Binary Integration *IEEE Transactions on Aerospace and Electronic Systems* **30**(1) 116-25
- [10] Richards M A 2005 *Fundamentals of Radar Signal Processing* New York: McGraw-Hill
- [11] Wang Y M, Ma J G, Fu Q, Zhuang Z W 2006 Research on integration detection of high-velocity moving target *Modern Radar* **28**(3) 24-7 (in Chinese)
- [12] Perry R P, Dipietro R C, Fante R L 2007 Coherent integration with range migration using Keystone formatting *In Proceedings of IEEE Radar Conference*
- [13] Su J, Xing M, Wang G, Bao Z 2010 High-velocity multi-target detection with narrowband radar *IET Radar Sonar and Navigation* **4**(4) 595-603
- [14] Zhang S S, Zeng T 2005 Dim target detection based on Keystone transform *In Proceedings of IEEE International Radar Conference* May 889-94
- [15] Xu J, Yu J, Peng Y, et al. 2011 Radon-Fourier transform for radar target detection I: generalized Doppler filter bank *IEEE Transactions on Aerospace and Electronic Systems* **47**(2) 1183-202
- [16] Xu J, Yu J, Peng Y-N, et al. 2011 Radon-Fourier Transform for Radar Target Detection, II: Blind Velocity Side lobe Suppression *IEEE Transactions on Aerospace and Electronic Systems* **47**(4) 2473-89
- [17] Xu J, Yu J, Peng Y-N, et al. 2012 Radon-Fourier transform for radar target detection III: Optimality and Fast Implementations *IEEE Transactions on Aerospace and Electronic Systems* **48**(2) 991-1004
- [18] Li-chang Qian, Jia Xu, Wen-feng Sun, Ying-ning Peng 2012 Blind Speed Side Lobe Suppression in Radon-Fourier Transform Based on Radar Pulse Recurrence Interval Design *Journal of Electronics & Information Technology* **34**(11) 2608-14 (in Chinese)
- [19] Lichang Qian, Jia Xu, Wenfeng Sun, et al. 2012 CLEAN based blind velocity side lobe (BSSL) suppression in the Radon Fourier Transform (RFT) for multi-target detection *Proc. of 2012 IEEE 12th International Conference on Computer and Information Technology* 490-5

Authors

	<p>Qian Chen, born on March 16, 1975, China</p> <p>Current position, grades: pursuing his Ph.D. degree in Beijing University of Science and Technology.</p> <p>University studies: B.S. degree from University of Electronic Science and Technology of China, in 1996, and the M.S. degree from Shanghai Radio Equipment institute, in 1999, China.</p> <p>Experience: He joined in the Shanghai Radio Equipment Research Institute in 1999, and has been a vice director.</p> <p>Scientific interest: are signal process, automobile anti-collision and radar system. He has been long engaged in short-range radar technology research.</p>
	<p>Junhao Liu, born on February 12, 1988, China</p> <p>University studies: B.S. degree in communication engineering from Nanjing University of Science & Technology, Nanjing, China, in 2011. He received the M.S. degree in 2014 from Shanghai Academy of Spaceflight Technology, Shanghai, China.</p> <p>Experience: He joined Shanghai Radio Equipment Research Institute, China, in 2014, where he has been engaged in research on weak signal processing, and short-range radar system.</p>
	<p>Chaowei Fu, born on May 21, 1985, China</p> <p>Current position, grades: a researcher at Shanghai Radio Equipment Research Institute, China.</p> <p>University studies: B.S. and M.S. degrees in engineering of signal and information processing from Xidian University, Xi'an, China, in 2010.</p> <p>Scientific interest: SAR Imaging and Signal processing.</p>
	<p>Haitao Wang, born on August 13, 1978, China</p> <p>Current position, grades: senior engineer in Shanghai Radio Equipment Research Institute.</p> <p>University studies: B.S. degree in Shandong University, Jinan, Shandong, in 2000. He received the M.S. degree in 2003 from Shanghai Academy of Spaceflight Technology, Shanghai, China.</p> <p>Scientific interest: radar signal processing, radar system and Terahertz detection technology.</p>